Received Signal Strength based Bearing-only Robot Navigation in a sensor network field

Nikhil Deshpande, Edward Grant, Mark Draelos, and Thomas C. Henderson

Abstract—This paper presents a low-complexity, novel approach to wireless sensor network (WSN) assisted autonomous mobile robot (AMR) navigation. The goal is to have an AMR navigate to a target location using only the information inherent to WSNs, i.e., topology of the WSN and received signal strength (RSS) information, while executing an efficient navigation path. Here, the AMR has neither the location information for the WSN, nor any sophisticated ranging equipment for prior mapping. Two schemes are proposed, that utilize particle filtering based bearing estimation with RSS values from directional antennas in the WSN-AMR interaction. Real-world experiments demonstrate the effectiveness of the proposed schemes. In the basic node-to-node navigation scheme, the bearing-only particle filtering reduces trajectory length by 11.7% (indoors) and 15% (outdoors), when compared to using raw bearing measurements. The advanced scheme further reduces the trajectory length by 22.8% (indoors) and 19.8% (outdoors), as compared to the basic scheme. The mechanisms exploit the low-cost, low-complexity advantages of the WSNs to provide an effective method for map-less and ranging-less navigation.

Index Terms—WSN-assisted navigation, received signal strength, particle filtering, bearing estimation

I. INTRODUCTION

Navigation of autonomous mobile robots (AMRs) in unknown and unstructured environments is confronted with a three-tier challenge: (i) identification of target locations, (ii) planning trajectories to identified locations, and (iii) executing the planned trajectories. Several research studies have explored the solutions to this challenge, either with expensive technology, such as laser range-finders and global positioning systems (examples in [20]), or with sophisticated planning algorithms with high computational complexity [18]. Wireless sensor networks (WSNs) deployed *apriori* in the environment provide a wealth of information regarding the state of the environment, e.g., seismic, magnetic, thermal or visual [1]. AMRs interacting with the distributed WSNs to navigate a region has been the topic of extensive research as well [2], [3], [7]. The AMRs utilize the information from the WSN to coordinate their behaviors, and have been used in applications including area coverage, search-and-rescue, target detection and tracking, cooperative transport, etc. [9], [10],

Nikhil Deshpande (nikhil.deshpande@iit.it) is with the Department of Advanced Robotics, Istituto Italiano di Tecnologia, Genova, Italy.
Edward Grant (egrant@ncsu.edu) is with the Department of Electrical and Computer Engineering, North Carolina State University, Raleigh, NC, USA.
Mark Draelos (mark.draelos@duke.edu) is with the School of Medicine, Duke University, Durham, NC, USA.
Thomas C. Henderson (tch@utah.edu) is with the School of Computing, University of Utah, Salt Lake City, UT, USA.

[16]. Through this cooperative interaction, the AMRs can effectively address the three-tier challenge. The research in this paper presents a novel approach to utilizing this WSN-AMR interactive navigation.

Navigation of AMRs in a WSN-covered region has been a subject of extensive research over the years. The research follows three main perspectives:

1) Mapping/Localizing for navigation: The WSN topology is used to map the navigation environment (similar to SLAM) and/or localize the WSN nodes which then assist the navigating AMR. Authors in [2] describe a Value-Iteration based probabilistic method for navigation. The transition probabilities at each WSN-node guide the AMR, and must be pre-assigned by an AMR that traverses the network several times before. Authors in [3] implement a two-step scheme: (i) the WiFi in the environment is first recorded for an RSS map; (ii) the AMR navigates the region using a perceptual model combining the live and the pre-recorded RSS data. Twigg et al. [21] demonstrate a combination of exploration and navigation to determine local RSS gradients while navigating towards the signal source.

2) Navigation with global positioning information: Known locations of WSN nodes, through technology (GPS) or algorithms (as above), informs the AMR as it navigates in the WSN-covered region. Li et al. [10] show the ability of WSNs in acting as guides to navigate AMRs using an artificial potential field based method - repulsion from "dangerous" (obstacle) sites and attraction to "goal" sites. The scheme utilizes GPS coordinates for the sensor node locations to assign the artificial potentials.

3) Navigation without location information: This perspective involves the AMR interacting with the WSN in real-time while navigating to desired target locations in unknown areas. The authors in [16] propose artificial gradients in the WSN that assist the navigating AMR. Similarly, Jiang et al. [9] present an RSS-based gradient in the WSN and a WSN-assisted navigation scheme for the AMR.

Yet, most of the prior art employs methods which are expensive, either in terms of: (i) technology [5], (ii) computation [18], (iii) time [2], [9], or (iv) economics [11].

In contrast to this prior research, the novel research explores the combination of low-complexity, probabilistic methods with low-cost hardware technologies to allow the AMR to navigate

a WSN field in an online manner, i.e., with and/or without an initialization phase. Two schemes are presented:

1) A basic scheme, where the AMR estimates the bearing to a neighboring WSN node. Received signal strength (RSS) values from the node are used to estimate the bearing. This allows the AMR to implement *node-to-node* navigation in an online manner, without requiring any initialization or setup phase.

2) An advanced scheme, where the AMR utilizes the RSS values from all the nodes in its neighborhood to estimate an overall bearing and thereby its next way-point in the neighborhood. This allows the AMR to execute *network* navigation trajectories by utilizing a prior initialization phase of the WSN.

This paper presents bearing-only methods of AMR navigation using RSS and online particle filtering. To be sure, integrating RSS measurements into a particle filter is not a novel approach. Ozdemir et al. [14] present the utility of particle filtering in overcoming the uncertainty in wireless communication channels, as well as the limitations of low-cost sensor nodes while tracking targets in a WSN field. The related research in [4] discusses the use of a distributed particle filter where the WSN nodes maintain particles of possible target trajectories. Liu et al. [11] show the use of a particle filter mechanism based on RSS values in an indoor RFID field. The scheme requires the robot to traverse the region in a training phase to build a fingerprint map of RSS values at various locations. Lu et al. [12] present a similar fingerprinting-based mechanism to generate a database of RSS values in a WiFi field. The particle filter is used to process the position estimate of the vehicle based on the database look-up and a constant velocity model.

This research presents novel methods wherein neither the location information for the AMR or the WSN, nor any ranging or prior mapping information in the WSN field, are required. They do not require the AMR to explore the region in determining local RSS gradients, nor do they require the localization of the WSN prior to navigating the field. They allow the AMR to come online and navigate towards a target immediately upon being introduced in the WSN field. The schemes do have certain limitations, which are noted later in the paper. As is the case with different navigation schemes, the choice shall depend on which parameter is critical for particular cases: cost, complexity, technology, or time.

II. System Description

Prior investigation by the authors in [6] and [7] demonstrated algorithms for optimized AMR trajectories in WSN-assisted navigation. In [7], the algorithms were shown to perform significantly better than [9], [10], [16]. One of the main points noted was that RSS provides enough information so that the AMR can traverse the field while interacting with the WSN as it moves, i.e., online, without a setup phase. Obtaining bearing information from RSS simplifies the task of the AMR in determining the next waypoint [21]. It is

advantageous because it: (i) is readily obtained using low-cost directional antennas and a simple triangulation scheme, (ii) can be obtained in an online manner, without requiring prior setup or initialization, and (iii) facilitates the online localization of the neighborhood of the AMR, as done in [7], instead of requiring to localize the complete network in a prior initialization step. These advantages are utilized in a bearing-only approach to RSS-based navigation planning in the presented schemes.

As shown in Fig. 1b, the RSS at the directional antenna is a function of the angle of the signal. Based on the radiation pattern of the directional antennas, the AMR platform has 3 of them in a 120° offset positioning, as seen in Fig. 1a. A triangulation method is then used to approximate the raw bearing θ of each node, using the angles at each of the directional antennas (Fig. 2a), similar to the method in [13]. The cost of the antennas is \$50 each [15]. This is considerably less expensive as compared to on-board GPS devices, costing upwards of \$500 [13]. The TMote Sky motes, having on-board omni-directional antennas, are used as network nodes - the communication parameters are noted in Table II.
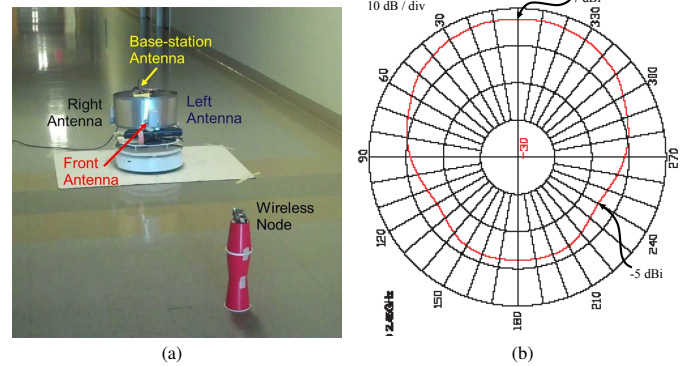

Fig. 1. Directional Antenna Setup and Radiation Pattern (from [15]).

III. Particle Filtering Algorithm for Bearing Estimation

In order to characterize the bearing measurement using the raw RSS values, trials were conducted with the AMR and a stationary node at three separate distances: $5'$, $15'$, and $25'$. At each distance, the AMR was rotated "in place" counter-clockwise for the full 360°, with RSS being recorded every 30°. Figure 2b shows the error in bearing measurements for the stationary node using the triangulation method, averaged over 100 samples. Clearly, some form of post-processing and filtering of the bearing data was required to overcome these errors, to allow efficient navigation.

The *particle filter* algorithm (PFA), a non-parametric implementation of the *Bayes filter* algorithm [20], is used to form the posterior estimation of the neighbor-node bearing. PFA allows the estimation process to account for factors impacting the RSS measurements that make them non-linear, e.g., multi-path effects, interference, shadow fading, etc. [8]. Due to its online nature, the filter recursively updates its estimation of

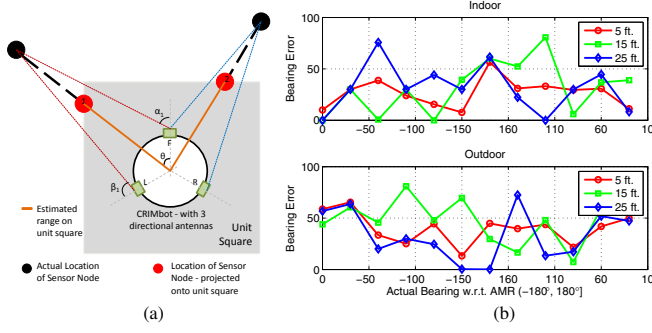(a)   (b)

Fig. 2. Triangulation-based bearing estimation and Bearing characterization statistics

the neighbor-node bearing. The introduced variables are noted in Table I.

Table I
VARIABLES IN PARTICLE FILTERING ALGORITHM.

Variable	Description
$\mathfrak{X}_t$	Set of N particles $x_t^{[n]}$ ($n = 1, 2,..., N$), hypotheses of the bearing estimate at time t. Each $x_t^{[n]}$ ($n \in N$) is given as $[r \; \theta]^T$. r is the range and θ is the bearing.
$w_t^{[n]}$ ($n \in N$)	Importance weight assigned to each particle.
z_t	Current measurement of the state, denoted as $[r \; \theta]^T$.
u_t	Control input to the AMR at time t, $[d \; \phi]^T$. d is the commanded travel and ϕ is the commanded turn. It is used as the odometry update.
$[\dot{d} \; \dot{\phi}]^T$	Commanded linear and angular velocities.

In order to satisfy the Markov assumption of the Bayesian filtering process, the range information must assist in the state update of the *prior* pdf of the bearing particle, incorporating the odometry update. But for the execution of the navigation, the AMR does not require range information. Therefore, the measurement update step excludes it. For ranging-less implementation, a constant neighborhood of the AMR is considered (a unit square - 1 m x 1 m) around itself (Fig. 2a).

$\mathfrak{X}_0$ is initialized to a set of uniform randomly distributed values over the interval $[-180^{\mathrm{o}}, 180^{\mathrm{o}})$ for θ, and u_0 and r as zero, the following procedure is used to implement the PFA.

1) **State Update:** The bearing particles are updated based on the control input given to the AMR. The process model used in this step is given by:

$$x_t^{[n]} = x_{t-1}^{[n]} - u_t + \omega_t \qquad \forall \; n \quad particles \quad (1)$$

The process noise variable ω_t implies that the AMR's odometry update u_t is trusted with an associated uncertainty. The uncertainty is generally a variable drawn from a normal distribution.

2) **Measure:** The new state measurement z_t consisting of the bearing (and the range information) from the 3-antenna triangulation method noted earlier.

3) **Measurement Update:** The importance weight of each particle incorporates the new measurement into the state's representation. Following *Bayes'* rule, a measurement model $p(z_t|x_t^{[n]})$ relates the state to the measurement. In this paper, a Gaussian relationship sufficiently demonstrates the improvement in efficiency. The weights for each particle are updated using the equation:

$$w_t^{[n]} = e^{-\frac{z_t - x_t^{[n]}}{\eta}} + \epsilon \qquad (2)$$

ϵ is a small value ('> 0') to ensure $w_t^{[n]} > 0$ always. η is the uncertainty with which z_t is trusted. A high η value indicates that z_t is very noisy, while a low η value implies greater z_t accuracy. Also, as noted earlier, the 'r' term in z_t is ignored while updating the weights.

4) **Resample:** The 'Select with Replacement Resampling' algorithm (pp. 33, [17]) is considered in this research. The probability that a particle will propagate to the next iteration is equal to its importance weight, implying that particles with higher weight have a higher probability of being copied multiple times for the next iteration. The count N of the particles is the same for every iteration.

A. Characterization of PF-based Bearing Estimation

Figure 3a shows a visualization of the PFA as it is applied in hardware, for a node held stationary at 45° from the AMR. As can be seen, the particles start off in all possible directions. As the number of observations increases, the particles get resampled and the estimated bearing converges to the best estimate. Figure 3b shows the convergence of the bearing estimate from the PFA as compared to the raw bearing observations using triangulation, over 9 time steps.

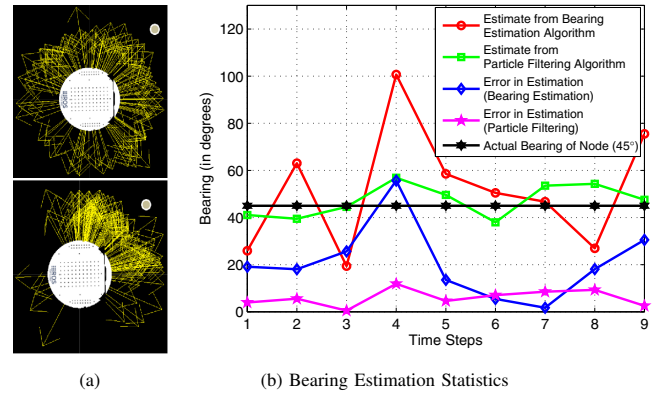(a)   (b) Bearing Estimation Statistics

Fig. 3. Characterization of PF-based Bearing Estimation.
(a) The images show the top-view of the AMR with the particles around it and the node ('brown' blob at 45°) near it. The particles are depicted as 'yellow' arrows with the arrow head pointing to the bearing estimate of that particle. The top image is at time step 0 instant, and the bottom image is at the end of the trial.

From Fig. 3b, it is noted, that the mean error in the bearing estimate using the PFA is non-zero, 5.98^{o}. Since the Gaussian model does not ideally model the noise and the interference in the directional antennas, an average error of zero would not be possible. But as is seen in the actual experiments, this model

lends itself sufficiently in significantly improving navigation efficiency.

B. Analysis Parameters

To enhance the quality of the RSS readings, the mean RSS value at each antenna is calculated over 50 communication packets, with an inter-packet interval of 100 ms. Table II lists the various parameters used during experimentation. The AMR is assumed to have reached a *target-node* when its RSS value at the AMR is above the preset threshold value of -40 dBm. The values were computed after extensive trials in the

Table II
PARTICLE FILTERING - PARAMETER CONFIGURATION

WSN Transmit Power (P_t)		-3 dBm	
Number of RSS packets (m)		50	
Inter-packet Interval (t)		100 ms	
Path Loss Exponent		1.6 (Indoors), 2.4 (Outdoors)	
Number of Particles		250	
ω_t	0.1^c	η	$(^3/_4)\pi$
$\dot{d}$	0.25 m/s	$\dot{\phi}$	35 deg./s

experiment scenarios, following the suggestions in [8], [19], [20]. Performance metrics are used to analyze the effectiveness of the methods. Two of them are stated here:

1) Travel-Distance Ratio: is measured as the ratio of the actual distance traveled by the AMR to the Euclidean distance between the start location and the target location. This impacts its energy expenditure as well as its quick-response capabilities.

2) Number of Way-points: is the number of intermediate locations required by the AMR in its trajectory from the start location to the target. The intermediate locations are points where the AMR communicates with WSN nodes to compute the next way-point. This impacts the WSN-AMR communication overhead during navigation.

IV. BASIC NAVIGATION SCHEME

In the basic scheme, the AMR executes node-to-node navigation. In the hardware implementation, the AMR incrementally moves towards the nodes, estimating the bearing after traveling a specific distance in the direction of the previous bearing estimate. The navigation procedure followed is:

1) The PFA from section III estimates the bearing θ for the neighbor-node.

2) The way-point is then issued in the form of control input $[d\ \phi]^T$, where ϕ is simply the estimated bearing θ. For these experiments, d is maintained a constant 0.3 m (~ 1 ft.).

It is noted that in the basic scheme, there is no initialization and setup phase with the WSN. The AMR can initiate navigation to the nodes immediately upon deployment. A sample experiment is shown in Fig. 4a, comparing the trajectories adopted by the two methods – with and without PFA[1]. As

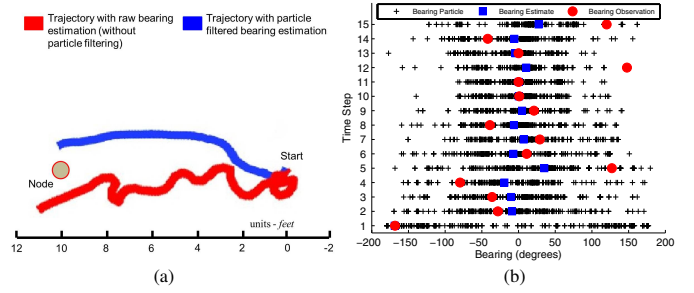[1]Initially, the AMR has its heading away from the node.

Fig. 4. Basic Navigation Scheme Trajectory - Comparative Analysis.
(b) The 'Bearing Estimate' is calculated as the weighted mean of all the resampled particles as mentioned in section (III). The 'Bearing Observation' is the latest raw bearing obtained using triangulation.

is observed, without PFA, the AMR takes more time steps and travels a longer, more tortuous route than the one using the PFA. Figure 4b details the estimation of the posterior distribution of the bearing variable over time. The distribution of the particles at time step 1 confirms that the AMR begins with its heading opposite to the node. As the AMR turns around and traverses towards the stationary node, the particles begin to cluster around the best estimate of the bearing, which would be in front of the AMR, around 0°. In contrast, the raw estimates calculated without PFA - annotated on the same figure at the respective time steps - show low convergence properties.

Table III summarizes the statistics for the basic navigation scheme experiments using a single node. The experiments were conducted indoors and outdoors for three different distances between the AMR and the node - $5'$, $10'$, and $15'$. At each distance, two trial runs were conducted and the averaged readings are reported here.

V. ADVANCED NAVIGATION SCHEME

As seen earlier, the basic navigation scheme is improved significantly by using the bearing-only PFA. But it does not utilize the inherent information in a deployed WSN, which can assist the AMR in further optimizing the trajectory. The advanced network navigation scheme is introduced which relies on a prior initialization phase of the WSN for the information of the target location. The 'Interpolation-based' navigation method introduced in [7] is utilized. The method is described here in brief:

1) In the WSN field, a *Pseudo-Gradient* (P-G) is generated (P-G algorithm, [6]), that has its peak closest to a target in the region.

   a) The node closest to the target marks itself as a *target-node* and initiates a packet exchange via a flooding mechanism[2].

   b) A magnitude (termed *pseu_g*) is assigned to each sensor node. This is a function of the node's communication distance (in terms of hop-count and

[2]A target could be an event (seismic, fire, chemical leak, etc.) or a moving entity. The nodes are assumed to be capable of sensing the target. This artifact shall be explored in a separate paper.

TABLE III
BASIC NODE-TO-NODE NAVIGATION - WITH AND WITHOUT PARTICLE FILTERING

Setting	Travel-Distance Ratios				Number of Way-points			
	Indoor		Outdoor		Indoor		Outdoor	
Method	without PFA	with PFA	without PFA	with PFA	without PFA	with PFA	without PFA	with PFA
5'	1.94	1.77	1.68	1.37	15	10	14	8
10'	1.87	1.57	1.85	1.57	22	17	21	17
15'	1.79	1.64	2.04	1.81	30	26	32	28
Average	1.88	1.66	1.86	1.58	-	-	-	-

RSS) from the *target-node*. So, the *target-node* had the highest magnitude assigned to it.

The P-G is based on the WSN topology and RSS [6].

2) Once this initialization phase is over, the AMR is introduced in the WSN field and it generates way-points by interpolating the distribution of P-G in its immediate neighborhood. It uses the estimated bearings of the neighbor-nodes and *Implicit Surface Interpolation* [7]. This is a surface fit using the *pseu_g* values at the neighbor-nodes, which allows the AMR to compute a local neighborhood way-point. The overall trajectory from this method is shown to be shorter and more efficient than comparable existing methods in literature, as noted in [7]. Figure 5 shows the improvement in trajectory with the interpolation scheme, reproduced from [7].
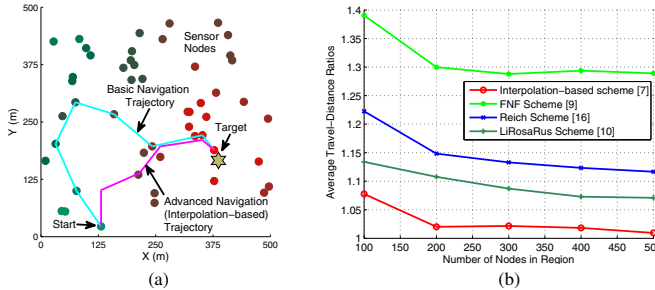

Fig. 5. Advanced 'Interpolation-based' navigation in simulation.
(a) Comparative AMR trajectories for Basic and Advanced navigation schemes. (b) Comparative performance of different navigation schemes.
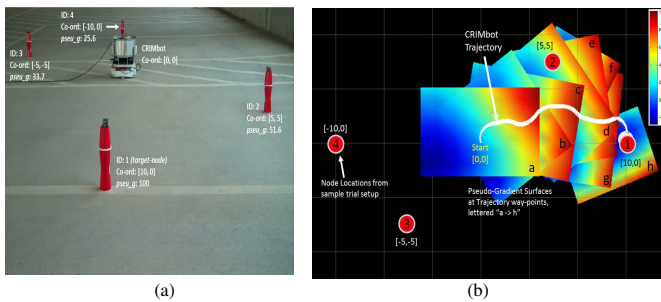

Fig. 6. Advanced navigation - sample trial setup (outdoor) and corresponding trajectory. All coordinates in *feet*.

The bearing estimate and range of each neighbor-node is obtained as shown in Fig. 2a. The bearing is then filtered using

the PFA. The P-G on the unit-square sub-neighborhood is then interpolated, and its peak becomes the next way-point.

The navigation procedure followed is:
1) The AMR obtains the *pseu_g*-values and the hop-counts of the neighbor-nodes.
2) It estimates the bearings of the neighbor-nodes with the PFA. Each neighbor-node has a PF associated with it.
3) The filtered bearing estimates and the range values (unit square) are then used to estimate the next neighborhood way-point using the interpolation method in [7].
4) The command $[d\ \phi]^T$ consists of the bearing ϕ and the travel distance d to this estimated way-point.

A sample trial setup is shown in Fig.6a. Figure 6b shows the trajectory for the AMR generated through the interpolated surface fits. The interpolation of the *pseu_g*-values is done with the AMR at the center of the surface fit. The next way-point is in the direction of the peak of the surface (highest value) at each location. It travels the fixed distance in that direction and repeats the above procedure for the next way-point.

Experiments were conducted using the above procedure with low-density networks - a 2-hop network indoors, and a 3-hop network outdoors. The hop-count values and the *pseu_g*-values were pre-assigned to the WSN nodes by executing the P-G algorithm, [6]. The actual distance between the AMR start location and the *target-node* was 30.4' (outdoor) and 24.5' (indoor). Figure 7 (a) and (b) show the sample trajectories in the two setups for the basic and the network navigation methods. The chosen layouts satisfied the necessary and sufficient condition of number of neighbor nodes for successful interpolation and way-point computation [7]. Three trials were conducted for the navigation methods in both the setups.

Table IV summarizes the statistics for these experiments.

VI. DISCUSSION

As is observed, in the basic scheme, particle filtering based navigation demonstrates superior performance. The PFA approach allows a 11.7% reduction indoors and a 15% reduction outdoors in the AMR Travel-Distance, over the values when PFA is not used. Similarly, the Number of Way-points is also reduced an average of 22.5% against the values when PFA is not used.

It is also clear that the advanced network navigation scheme performs significantly better than the basic navigation one. Here, even more pronounced reductions in metric values are

Table IV
COMPARISON OF BASIC AND NETWORK NAVIGATION METHODS (BOTH WITH PFA)

Setting	Travel-Distance Ratios				Number of Way-points			
	Indoor (2-hop)		Outdoor (3-hop)		Indoor (2-hop)		Outdoor (3-hop)	
Method	Basic	Network	Basic	Network	Basic	Network	Basic	Network
Trial 1	1.65	1.28	1.74	1.41	43	15	50	20
Trial 2	1.60	1.23	1.71	1.42	40	14	48	20
Trial 3	1.61	1.25	1.71	1.32	41	15	48	19
Average	1.62	1.25	1.72	1.38	41.3	14.7	48.7	19.7

(a) Indoor Setup

(b) Outdoor Setup

Fig. 7. Setup for navigation experiments - with basic and advanced schemes.

Table V
AMR RESPONSE TIMES COMPARISON (SECONDS)

	Basic (Single Node) Navigation			
	without PFA		with PFA	
	Indoor	Outdoor	Indoor	Outdoor
Calculated	180.7	282.8	146.2	221.0
Actual	184.4	287.3	148.4	223.2
	Advanced (Network) Navigation			
	Basic		Network	
	Indoor	Outdoor	Indoor	Outdoor
Calculated	336.3	428.1	266.7	353.9
Actual	338.1	429.8	286.8	367.4

observed. The Travel-Distance is reduced by 22.8% indoors, and 19.8% outdoors. The Number of Way-points is reduced by 64.41% indoors, and 59.5% outdoors. This also corroborates the simulation results in [7].

The overall response time of the AMR in arriving at the detected target is the *third* performance metric. Equation 3 presents the relationship.

$$T_{resp} = \sum_{i=1}^{P} n_i \cdot m_i \cdot t_i + \sum_{i=1}^{P} \frac{d_i}{\dot{d}_i} + \sum_{i=1}^{P} \frac{\phi_i}{\dot{\phi}_i} + P \cdot \varepsilon \quad (3)$$

Here, P is the number of way-points in the trajectory. n_i is the number of WSN neighbor-nodes at way-point i. ε accounts for computation time of a way-point (including any inter-communication between peripherals). Its value is set to 10 ms. The other variables are noted in Table II, and in sections IV and V separately. The average values of the calculated from (3) and the actual response times for the experiments are noted in Table V.

The response times show a trend similar to that of the other two metrics. With PFA, the basic navigation experiences a 19.5% reduction indoors, and a 22.3% reduction outdoors, in the actual response times averaged over $5'$, $10'$, and $15'$. For the advanced navigation, the actual response times reduce by 13.6% (indoors) and 14.5% (outdoors) over the basic scheme.

Limitations of the schemes

The significant gains obtained in the response times point to the clear advantages of the bearing-only, PF-based navigation schemes. Yet, evidently the schemes suffer from drawbacks.

1) The advanced navigation scheme has a higher response time than the basic navigation scheme. This is because the advanced scheme has to interact with multiple nodes as it navigates, instead of just one, as in the basic scheme.

2) The overall response times to navigate distances between 10 - 20 ft. are rather high. This is attributed to the communication overhead to mitigate the noisy RSS values.

3) The schemes do not have a way of avoiding obstacles, since they only have RSS sensors on-board.

Yet, these limitations are offset by the improvements offered by the schemes in: (i) reduced trajectory lengths thereby reduced energy expenditure, (ii) lower complexity, (iii) simpler technological requirements, and (iv) lower overall cost. The strategies allow online AMR navigation and can be readily adopted in WSN-assisted methods.

VII. CONCLUSIONS AND FUTURE WORK

In this paper, low-cost and low-complexity schemes were explored in WSN-assisted AMR navigation. Using an RSS-based, bearing-only, particle filtering mechanism, the two nav-

igation schemes demonstrated online navigation and efficient execution of trajectory, both with and without the requirement of an initialization phase. Real-world experiments with the schemes also corroborate the simulation results observed in [7]. The basic method is a naive node-to-node navigation implementation, important in cases where the AMR can communicate with only one neighbor-node. The advanced method takes advantage of the information in the WSN to improve its trajectory, but requires more communication overhead. The quantum of improvement in the trajectory length and the number of way-points has a direct impact on the overall response times of the AMR, presenting a reduction between 13.6% and 22.3%. The critical advantage of the schemes, in addition to these enhancements, is their capability of operating in environments without the need of global positioning, ranging, or prior mapping information.

In future research, two key aspects that shall be investigated are: (i) utilizing the RSS information for obstacle avoidance; one of the methods was discussed in [6], and (ii) decoupling the AMR motion from the RSS measurement and bearing estimation. This will allow for a more smooth and continuous trajectory execution. Some of the other important aspects that will be explored are: (i) including RSS-based ranging information without assuming its Gaussian distribution (similar to [18]), and (ii) testing the robustness to link and node failures during navigation. The investigation will include the analysis with presence of multiple targets and coordinated multiple AMR navigation as well.

REFERENCES

[1] I. F. Akyildiz, W. Su, Y. Sankarasubramaniam, and E. Cayirci, "Wireless Sensor Networks: A Survey," *Computer Networks*, vol. 38, pp. 393–422, 2002.

[2] M. A. Batalin, G. S. Sukhatme, and M. Hattig, "Mobile Robot Navigation using a Sensor Network," in *Proc. IEEE Intl. Conf. on Robotics and Automation, (ICRA '04)*, 2004, pp. 636–641.

[3] J. Biswas and M. Veloso, "WiFi Localization and Navigation for Autonomous Indoor Mobile Robots," in *Proc. IEEE Intl. Conf. on Robotics and Automation, (ICRA '10)*, May 2010, pp. 4379–4384.

[4] M. Coates and G. Ing, "Sensor Network Particle Filters: Motes as Particles," in *Proc. 13th IEEE/SP Workshop on Statistical Signal Processing*, Jul. 2005, pp. 1152–1157.

[5] P. Corke, R. Peterson, and D. Rus, "Localization and Navigation Assisted by Networked Cooperating Sensors and Robots," *Intl. Journal of Robotics Research*, vol. 24, no. 9, pp. 771–786, 2005.

[6] N. Deshpande, E. Grant, and T. C. Henderson, "Experiments with a "pseudo-gradient" algorithm for target localization using wireless sensor networks," in *Proc. IEEE Intl. Conf. on Multisensor Fusion and Integration for Intelligent Systems, (MFI 2010)*, Sept. 2010, pp. 74–79.

[7] ——, "Target-directed Navigation using Wireless Sensor Networks and Implicit Surface Interpolation," in *Proc. IEEE Intl. Conf. on Robotics and Automation, (ICRA '12)*, May 2012, pp. 457–462.

[8] A. Goldsmith, *Wireless Communications*. ©Cambridge University Press, 2005.

[9] J.-R. Jiang, Y.-L. Lai, and F.-C. Deng, "Mobile Robot Coordination and Navigation with Directional Antennas in Positionless wireless sensor networks," in *Proc. Intl. Conf. on Mobile Technology, Applications, and Systems, (Mobility '08)*, 2008, pp. 1–7.

[10] Q. Li, M. De Rosa, and D. Rus, "Distributed Algorithms for Guiding Navigation across a sensor network," in *Proc. 9th Intl. Conf. on Mobile Computing and Networking, (MobiCom '03)*, 2003, pp. 313–325.

[11] R. Liu, P. Vorst, A. Koch, and A. Zell, "Path Following for Indoor Robots with RFID Received Signal Strength," in *Proc. 19th Intl. Conf. on Software, Telecommunications and Computer Networks, (SoftCOM 2011)*, Sep. 2011.

[12] H. Lu, S. Zhang, X. Liu, and X. Lin, "Vehicle Tracking Using Particle Filter in Wi-Fi Network," in *Proc. IEEE 72nd Vehicular Technology Conference, (VTC 2010)*, Sep. 2010, pp. 1–5.

[13] N. Malhotra, M. Krasniewski, C.-L. Yang, S. Bagchi, and W. J. Chappell, "Location Estimation in Ad-Hoc Networks with Directional Antennas," in *Proc. 25th IEEE Intl. Conf. on Distributed Computing Systems, (ICDCS 2005)*, 2005, pp. 633–642.

[14] O. Ozdemir, R. Niu, and P. K. Varshney, "Tracking in Wireless Sensor Networks Using Particle Filtering: Physical Layer Considerations," *IEEE Transactions on Signal Processing*, vol. 57, no. 5, pp. 1987–1999, may 2009.

[15] Quatech. (2003) ACH2-AT-DP006 Directional Antenna. DPAC Technologies. [Online]. Available: http://www.quatech.com/catalog/accessories.php.

[16] J. Reich and E. Sklar, "Robot-Sensor Networks for Search and Rescue," in *Proc. IEEE Intl. Workshop on Safety, Security and Rescue Robotics*, 2006.

[17] I. M. Rekleitis, "A Particle Filter Tutorial for Mobile Robot Localization," Center for Intelligent Machines, McGill University, Tech. Rep. TR-CIM-04-04, 2004.

[18] P. Soriano, F. Caballero, and A. Ollero, "RF-based Particle Filter Localization for Wildlife Tracking by using an UAV," in *Proc. 40th Intl. Symp. on Robotics*, Mar. 2009, pp. 239–244.

[19] K. Srinivasan, M. A. Kazandjieva, S. Agarwal, and P. Levis, "The β-factor: Measuring Wireless Link Burstiness," in *Proc. 6th Intl. Conf. on Embedded Networked Sensor Systems, (SenSys '08)*, 2008, pp. 29–42.

[20] S. Thrun, W. Burgard, and D. Fox, *Probabilistic Robotics*. ©MIT Press, 2006.

[21] J. N. Twigg, J. R. Fink, P. L. Yu, and B. M. Sadler, "RSS Gradient-Assisted Frontier Exploration and Radio Source Localization," in *Proc. IEEE Intl. Conf. on Robotics and Automation, (ICRA '12)*, 2012, pp. 889–895.